ResearchGate

See discussions, stats, and author profiles for this publication at: https://www.researchgate.net/publication/45459925

Free Energy Perturbation Simulation on Transition States and High-Activity Mutants of Human Butyrylcholinesterase for (-)-Cocaine Hydrolysis

ARTICLE *in* THE JOURNAL OF PHYSICAL CHEMISTRY B · AUGUST 2010

Impact Factor: 3.3 · DOI: 10.1021/jp104989b · Source: PubMed

CITATIONS
15

READS
29

6 AUTHORS, INCLUDING:

Lei Fang
University of Kentucky
20 PUBLICATIONS **190** CITATIONS
SEE PROFILE

Daquan Gao
University of Kentucky
26 PUBLICATIONS **813** CITATIONS
SEE PROFILE

Available from: Lei Fang
Retrieved on: 24 January 2016

NIH Public Access
Author Manuscript
J Phys Chem B. Author manuscript; available in PMC 2011 August 26.

Published in final edited form as:
J Phys Chem B. 2010 August 26; 114(33): 10889–10896. doi:10.1021/jp104989b.

Free-Energy Perturbation Simulation on Transition States and High-Activity Mutants of Human Butyrylcholinesterase for (−)Cocaine Hydrolysis

Wenchao Yang[1,2,a], **Yongmei Pan**[2,a], **Lei Fang**[2], **Daquan Gao**[2], **Fang Zheng**[2], and **Chang-Guo Zhan**[2,*]

[1] Key Laboratory of Pesticide & Chemical Biology of Ministry of Education, College of Chemistry, Central China Normal University, Wuhan 430079, P. R. China

[2] Department of Pharmaceutical Sciences, College of Pharmacy, University of Kentucky, 789 South Limestone, Lexington, KY 40536

Abstract

A unified computational approach based on free energy perturbation (FEP) simulations of transition states has been employed to calculate the mutation-caused shifts of the free energy change from the free enzyme to the rate-determining transition state for (−)-cocaine hydrolysis catalyzed by the currently most promising series of mutants of human butyrylcholinesterase (BChE) that contain the A199S/A328W/Y332G mutations. The FEP simulations were followed by Michaelis-Menten kinetics analysis determining the individual k_{cat} and K_M values missing for the A199S/F227A/A328W/Y332G mutant in this series. The calculated mutation-caused shifts of the free energy change from the free enzyme to the rate-determining transition state are in good agreement with the experimental kinetic data, demonstrating that the unified computational approach based on the FEP simulations of the transition states may be valuable for future computational design of new BChE mutants with a further improved catalytic efficiency against (−)-cocaine.

Keywords

Butyrylcholinesterase; cocaine; transition state simulation; free energy perturbation; enzyme mutant design

Introduction

Cocaine is a well-known drug of abuse.[1,2,3] There is still no approved medication specific for cocaine abuse treatment. The disastrous medical and social consequences of cocaine abuse have made the development of an anti-cocaine medication a high priority.[4,5] It would be an ideal anti-cocaine medication to accelerate cocaine metabolism producing biologically inactive metabolites *via* a route similar to the primary cocaine-metabolizing pathway, *i.e.* cocaine hydrolysis catalyzed by butyrylcholinesterase (BChE) in plasma.[4,6,7,8,9,10]

*Correspondence: Chang-Guo Zhan, Ph.D., Professor, Department of Pharmaceutical Sciences, College of Pharmacy, University of Kentucky, 789 South Limestone, Lexington, KY 40536, TEL: 859-323-3943, FAX: 859-323-3575, zhan@uky.edu.
[a]These authors contributed equally to this work.

Supporting Information Available. The MD parameters used in this study; Table for the individual ΔG_E or ΔG_{TS1} values obtained from the FEP simulations using five different initial structures associated with different snapshots of the MD trajectory. This material is available free of charge *via* the Internet at http://pubs.acs.org.

NIH-PA Author Manuscript
NIH-PA Author Manuscript
NIH-PA Author Manuscript

NIH-PA Author Manuscript

NIH-PA Author Manuscript

NIH-PA Author Manuscript

Unfortunately, wild-type BChE has a low catalytic efficiency against naturally occurring (−)-cocaine (k_{cat} = 4.1 min^{-1} and K_M = 4.5 μM).[11,12,13,14,15]

For anti-cocaine medication development, it is interesting to design a mutant of human BChE, which may be regarded as a cocaine hydrolase (CocH), with a significantly improved catalytic activity against (−)-cocaine. It has been known that computational design of a high-activity enzyme mutant is extremely challenging, particularly when the chemical reaction process is rate determining for the enzymatic reaction.[16,17,18] Generally speaking, for computational design of a mutant enzyme with an improved catalytic activity for a given substrate, one needs to design possible amino acid mutations that can accelerate the rate-determining step of the catalytic reaction process[12,19,20] while the other steps are not slowed down by the mutations. The detailed catalytic reaction pathway for BChE-catalyzed hydrolysis of (−)cocaine was uncovered by extensive molecular dynamics (MD) simulations[12,19] and reaction coordinate calculations[19,20] using quantum mechanics (QM) and hybrid quantum mechanics/molecular mechanics (QM/MM). It has been known[12,16,19,21] that the rate-determining step of (−)-cocaine hydrolysis catalyzed by the A328W/Y332A and A328W/Y332G mutants is the first step of the chemical reaction process. Therefore, starting from the A328W/Y332A or A328W/Y332G mutant, rational design of BChE mutants against (−)-cocaine has been focused on decreasing the energy barrier for the first reaction step without significantly affecting the other reaction steps.[21,22,23,24]

The most promising high-activity mutants of BChE discovered so far contain the A199S/A328W/Y332G mutations.[22] In particular, the high activity (k_{cat} = 3060 min^{-1} and K_M = 3.1 μM)[25] of our previously discovered A199S/S287G/A328W/Y332G mutant[21] against (−)-cocaine has been validated *in vitro* and *in vivo* by an independent group of scientists, *i.e*. Brimijoin *et al.*,[26] who concluded that this mutant is "*a true CocH with a catalytic efficiency that is 1,000-fold greater than wild-type BChE*".[26] Brimijoin *et al.* fused this BChE mutant at its C-terminus with human serum albumin to extend the plasma half-life of the enzyme and found that the BChE mutant (or CocH) fused with human serum albumin can selectively block cocaine toxicity and reinstatement of drug seeking in rats.[26] All of the experimental data reported by Brimijoin *et al.*[26] strongly supported the potential therapeutic value of our designed and discovered A199S/S287G/A328W/Y332G mutant of human BChE, and they concluded that the enzyme treatment with this mutant "*was well tolerated and may be worth exploring for clinical application in humans*".[26] Further, it has been demonstrated[23] that the A199S/F227A/S287G/A328W/Y332G mutant has an even higher catalytic efficiency against (−)-cocaine (k_{cat} = 5700 min^{-1} and K_M = 3.1 μM) and that it can more potently protect animals from the cocaine toxicity.

It should be pointed out that, within this promising series of BChE mutants (including the A199S/A328W/Y332G, A199S/F227A/A328W/Y332G, A199S/S287G/A328W/Y332G, and A199S/F227A/S287G/A328W/Y332G), different mutants were designed by using different computational approaches to virtually screen the transition states associated with various hypothetical mutants.[21,22,23] Thus, no unified computational approach has been employed to examine the structure-activity correlation for all of these BChE mutants. In addition, there are no individual k_{cat} and K_M values available for the A199S/F227A/A328W/Y332G mutant against (−)-cocaine.

In the present study, we examined the structure-activity correlation for this series of BChE mutants by using a unified FEP-TS approach,[22] *i.e*. the free energy perturbation (FEP) simulations on the rate-determining transition state (TS1), *i.e*. the transition state for the first step, of the enzymatic reaction for each mutant. An approximation used in the FEP-TS approach is that the perturbation associated with the simulated amino acid mutation does not

NIH-PA Author Manuscript

NIH-PA Author Manuscript

NIH-PA Author Manuscript

significantly affect the lengths of the transition bonds, *i.e*. the gradually forming/breaking covalent bonds during the reaction step. The approximation is reasonable so long as the mutated amino acid residue does not directly interact with the atoms involved in the transition bonds. The FEP simulations were carried out to predict the mutation-caused shifts of the free energy change from the free enzyme to the rate-determining transition state for (−)-cocaine hydrolysis catalyzed by the BChE mutants. For comparison between computational and experimental data, we also determined the individual k_{cat} and K_M values missing for the BChE mutant in this series against (−)-cocaine by carrying out the Michaelis-Menten kinetics analysis. The FEP-based computational results are in good agreement with the experimental kinetic data, suggesting that the unified computational approach based on the FEP simulations of the transition states may be valuable for future computational design of new BChE mutants with a further improved catalytic efficiency against (−)-cocaine.

Methods

Computational studies

The general computational strategy and protocol for FEP simulations on a transition state of the enzymatic reaction have been described and rationalized elsewhere.[22] Prior to FEP simulations on each mutation, we first performed molecular dynamics (MD) simulations on the unperturbed free enzyme structure and the first transition state (TS1) structure. The initial structures of both the free enzyme and transition state TS1 used in the MD simulations were prepared based on our previous MD simulations[16,22] on the structures of wild-type BChE and its mutants, that were derived from the X-ray crystal structure.[27] Each MD simulation was carried out for at least 1 ns or longer until a stable MD trajectory was obtained. The FEP simulations started from the MD-simulated structures of the unperturbed systems. The schematic structure of the transition state TS1 is shown in Figure 1. The detail of the determination of the TS1 structure has been described previously.[21,22,23] Briefly, the key features of the TS1 structure involve the partially formed and partially broken covalent bonds, *i.e.* transition bonds denoted in this paper formed within the catalytic triad (including Ser198, Glu325, and His438) and the transition bond between the hydroxyl oxygen of Ser198 side chain and a carbonyl carbon of the (−)-cocaine. The transition bonds were restrained by defining the bond length parameters of new atom types of specific atoms in the TS1 structure based on the geometry obtained from the reaction coordinate calculations on the (−)-cocaine hydrolysis catalyzed by wild-type BChE.[19] The partial atomic charges of the non-standard residues in the TS1 structures were calculated by using the RESP protocol implemented in the Antechamber module of the Amber7 package[28] following electrostatic potential (ESP) calculations at *ab initio* HF/6-31G* level using the Gaussian03 program.[29] The geometries used in the ESP calculations were those obtained from the previous reaction coordinate calculations.[19] The charges of the residue atoms of the TS1 structure were those from the standard Amber force field used in the Amber7 package. The determined RESP charges and force-field parameters are provided in Supporting Information.

All of the MD simulations were performed by using the Sander module of Amber7 package with the same procedures as described in our previous computational studies.[21,22] For free enzyme structures, the +1 charge of the enzyme was neutralized by adding one chloride counterion. For TS1 structure, the +2 charge of the system was neutralized by adding two chloride counterions. Both the free enzyme and TS1 structures were solvated in a rectangular box of TIP3P water molecule[30] with a minimum solute-wall distance of 10 Å. The solvated systems were carefully equilibrated and fully energy-minimized. These systems were gradually heated from T = 10 K to T = 298.15 K in 40 ps before running the MD simulation at T = 298.15 K for 1 ns or longer, making sure that we obtained a stable MD trajectory for each of the simulated structures. The time step used for the MD

NIH-PA Author Manuscript

NIH-PA Author Manuscript

NIH-PA Author Manuscript

simulations was 2 fs. Periodic boundary condition was used in the NPT ensemble at T = 298.15 K using Berendsen temperature coupling and P = 1 atm with isotropic molecular-based scaling.[31] The SHAKE algorithm[32] was used to fix all covalent bonds containing hydrogen atoms. The non-bonded pair list was updated every 25 steps. The particle mesh Ewald (PME) method[33] was used to treat long-range electrostatic interactions. 10 Å was used as the non-bonded cutoff.

The outcomes of the FEP simulations on the mutations of both the free enzyme and TS1 structures can be used to predict the mutation-caused change of the catalytic efficiency for BChE-catalyzed hydrolysis of (−)-cocaine. Depicted in Figure 2 are the free energy changes associated with two reaction systems: one is the (−)-cocaine hydrolysis catalyzed by a BChE mutant (or the wild-type), denoted by Enzyme 1 or E(1); the other is the (−)-cocaine hydrolysis catalyzed by another BChE mutant, denoted by Enzyme 2 or E(2). As seen in Figure 2, the catalytic efficiency, *i.e.* $k_{cat}(i)/K_M(i)$, for the (−)-cocaine hydrolysis catalyzed by enzyme E(i) is determined by the Gibbs free energy change $\Delta G(i)$ of the reaction system from E(i) plus substrate S, *i.e.* (−)-cocaine, to the corresponding rate-determining transition state TS1(i). $\Delta G(i)$ is the sum of the enzyme-substrate binding free energy $\Delta G_{ES}(i)$ and the activation free energy $\Delta G_{av}(i)$:

$$\Delta G(i)=\Delta G_{ES}(i)+\Delta G_{av}(i),\ \ i=1 \text{ and } 2. \tag{1}$$

When a mutation on an amino acid residue can change the enzyme from E(1) to E(2), we want to know the corresponding free energy change from $\Delta G(1)$ to $\Delta G(2)$ for the computational design of the high-activity mutants of the enzyme. There are two possible paths to determine the free energy change $\Delta\Delta G(1\rightarrow 2) \equiv \Delta G(2) - \Delta G(1)$. One path is to directly calculate $\Delta G_{ES}(i)$ and $\Delta G_{av}(i)$ associated with E(1) and E(2), which is very computationally demanding in terms of the level of theory. For an alternative path, the relatively less-demanding FEP simulations allow us to estimate $\Delta\Delta G(1\rightarrow 2)$ by determining the free energy changes ΔG_E and ΔG_{TS1} from E(1) to E(2):

$$\Delta\Delta G(1 \rightarrow 2)=\Delta G_{TS1} - \Delta G_E \tag{2}$$

where ΔG_E and ΔG_{TS1} are the free energy changes from E(1) to E(2) for the free enzyme and TS1, respectively. ΔG_E and ΔG_{TS1} were estimated by performing the FEP simulations in the present study. By using the calculated $\Delta\Delta G(1\rightarrow 2)$, the ratio of the catalytic efficiency associated with E(2) to that associated with E(1) can be evaluated,

$$\Delta\Delta G(1 \rightarrow 2)= - RT\ln\frac{k_{cat}(2)/K_M(2)}{k_{cat}(1)/K_M(1)}. \tag{3}$$

Equation (3) can also be used to derive the experimental $\Delta\Delta G(1\rightarrow 2)$ value from the experimental ratio of the catalytic efficiency associated with E(2) to that associated with E(1).

We examined the above FEP-based computational approach for various mutations, including those associated with the following enzyme changes:

$$\text{A199S/A328W/Y332G} \rightarrow \text{A199S/F227A/A328W/Y332G} \tag{4}$$

NIH-PA Author Manuscript

NIH-PA Author Manuscript

NIH-PA Author Manuscript

A199S/A328W/Y332G → A199S/S287A/A328W/Y332G (5)

A199S/S287A/A328W/Y332G → A199S/S287G/A328W/Y332G (6)

A199S/S287G/A328W/Y332G → A199S/F227A/S287G/A328W/Y332G (7)

Equations (4) to (7) indicate that each mutation simulated in this study changes a larger side chain to a smaller one. We only carried out the FEP simulations on single mutations because the FEP simulations on simultaneous multiple mutations are expected to be less accurate. For the diminishing atoms during the perturbation simulation from a larger side chain to a smaller one, the dummy atoms were added to the perturbed residue to keep the number of atoms constant. Thus, some normal atoms in the starting structure were gradually mutated to the dummy atoms in the perturbed residue. For the dummy atoms, new atom type "DH" was given to the diminished hydrogen, atom type "DC" to the diminished carbon atom in the mutations, and atom type "DO" to the diminished oxygen atom in the mutations. The charges and the non-bond parameters of the dummy atoms were set to zero so that they did not have electrostatic or van der Waals interactions with other atoms. At the same time, all of the bond and angle parameters involving the dummy atoms were the same as their counterparts in the initial structure in order to keep the structural skeletons unchanged. The default choice (INTPRT = 0) was used to make sure that the bonded interactions of the dummy atoms were excluded from the final calculation on the total energy of the perturbed system. The FEP simulations (with a time step of 1 fs) were carried out by using the "fixed width window growth" method implemented in the Gibbs module of Amber7.[28]

To enlarge the phase space searched by the FEP calculation, for each perturbation, five different conformations were extracted from the stable MD trajectory with an interval of 100 ps (one snapshot per 100 ps). The equally distributed five snapshots of the simulated structure within the stable MD trajectory were used as the initial structures of the perturbation simulations. The finally calculated ΔG_{TS1} or ΔG_E value is the average of the ΔG_{TS1} or ΔG_E values associated with the various initial structures. Each initial structure was first energy-minimized for 1,000 cycles followed by 40 ps MD simulation for the heating and equilibration to obtain a better starting structure for the FEP calculation. The number of FEP windows and the number of the simulation steps for each window used in the present study are the same as those used in our previous studies on other BChE mutants.[22,24] For FEP calculations on all mutations, we used 51 windows ($\Delta\lambda = 0.02$), each window of the FEP simulation included 1,250 steps of equilibration and 1,250 steps for data collection, with both forward and backward directions in each FEP calculation. Thus, for the FEP simulation on each mutation, we performed the MD simulations for a total of 2,500 × 51 × 5 = 637,500 steps or 637.5 ps.

Experimental studies

[^{3}H](−)-cocaine (50 Ci/mmol) was purchased from PerkinElmer Life Sciences (Boston, MA). Human embryonic kidney 293T/17 cells were from ATCC (Manassas, VA). Dulbecco's modified Eagle's medium (DMEM) was purchased from Fisher Scientific (Fairlawn, NJ). 3, 3′, 5, 5′-Tetramethylbenzidine (TMB) was obtained from Sigma (Saint Louis, Missouri). Anti-BChE (mouse monoclonal antibody, Product # HAH002-01) was purchased from AntibodyShop (Gentofte, Denmark) and goat anti-mouse IgG HRP conjugate was from Zymed (San Francisco, CA).

NIH-PA Author Manuscript

NIH-PA Author Manuscript

NIH-PA Author Manuscript

We examined both the wild-type and mutant of human BChE at the same time under the same experimental condition; the wild-type was used a standard reference. The proteins (wild-type and mutant of BChE) were expressed in human embryonic kidney cell line 293T/17. Cells were grown to 80–90% confluence in 6-well dishes and then transfected by Lipofectamine 2,000 complexes of 4 μg plasmid DNA per each well. Cells were incubated at 37 °C in a CO_2 incubator for 24 hours and cells were moved to 60-mm culture vessel and cultured for four more days. The culture medium [10% fetal bovine serum in Dulbecco's modified Eagle's medium (DMEM)] was harvested for the BChE activity assays.

To measure (−)-cocaine and benzoic acid, the product of (−)-cocaine hydrolysis catalyzed by BChE, we used sensitive radiometric assays based on toluene extraction of [^{3}H](−)-cocaine labeled on its benzene ring.[34] In brief, to initiate the enzymatic reaction, 100 nCi of [^{3}H](−)-cocaine was mixed with 100 μl of culture medium. The enzymatic reactions proceeded at room temperature (25°C) with varying concentrations of (−)-cocaine. The reactions were stopped by adding 300 μl of 0.02 M HCl, which neutralized the liberated benzoic acid while ensuring a positive charge on the residual (−)-cocaine. [^{3}H]benzoic acid was extracted by 1 ml of toluene and measured by scintillation counting. Finally, the measured (−)-cocaine concentration-dependent radiometric data were analyzed by using the standard Michaelis-Menten kinetics so that the catalytic parameters (k_{cat} and K_M) were determined along with the use of an enzyme-linked immunosorbent assay (ELISA) protocol.[23]

Results and Discussion

In order to theoretically calculate the $\Delta\Delta G(1\rightarrow2)$ values and the catalytic efficiency changes associated with enzyme changes (4) – (7), we performed MD simulations on both the free enzyme and TS1 structures of the A199S/A328W/Y332G, A199S/S287A/A328W/Y332G, and A199S/S287G/A328W/Y332G mutants. Stable MD trajectories with the simulation time of 1 ns or longer were obtained for these structures. The equally distributed five snapshots of the MD-simulated free enzyme or TS1 structure of the A199S/A328W/Y332G mutant extracted from the stable trajectory with a time interval of 100 ps were used as the starting structures to carry out the FEP simulations for the enzyme changes A199S/A328W/Y332G → A199S/F227A/A328W/Y332G and A199S/A328W/Y332G → A199S/S287A/A328W/Y332G. The equally distributed five snapshots of the MD-simulated free enzyme or TS1 structure of the A199S/S287A/A328W/Y332G mutant extracted from the stable trajectory with a time interval of 100 ps were used as the starting structures to perform the FEP simulations for the enzyme change A199S/S287A/A328W/Y332G → A199S/S287G/A328W/Y332G. The equally distributed five snapshots of the MD-simulated free enzyme or TS1 structure of the A199S/S287G/A328W/Y332G mutant extracted from the stable trajectory with a time interval of 100 ps were used as the starting structures to carry out the FEP simulations for the enzyme change A199S/S287G/A328W/Y332G → A199S/F227A/S287G/A328W/Y332G. Important computational results are depicted in Figures 3 to 5 and summarized in Table 1. The more detailed energetic results are provided in Supporting Information.

In Table 1, the values of the root-mean-square fluctuation (RMSF) among the individual energy changes associated with different initial structures are given in parentheses. As seen in Table 1, the absolute values of the FEP-simulated ΔG_{TS1} and ΔG_E range from 4.98 to 8.58 kcal/mol, while the RMSF values range from 0.16 to 0.54 kcal/mol. The RMSF values of our FEP simulations are comparable to the previously reported fluctuation values associated with different independent FEP runs on a same system in other computational studies.[35,36,37] It should be pointed out that the RMSF values do not necessarily reflect the computational errors of the FEP calculations. According to Press *et al*.,[38,39] the standard

NIH-PA Author Manuscript

NIH-PA Author Manuscript

NIH-PA Author Manuscript

error (SE) value is dependent on both the number (N) of snapshots chosen in the FEP simulations and the RMSF of the calculated ΔG_{TS1} or ΔG_E values associated with all snapshots:

$$SE=\frac{RMSE}{\sqrt{N}}. \quad (8)$$

So, the SE values are all smaller than the corresponding RMSF values when N > 1. In general, Eq. (8) suggests that the more starting structures used in the FEP simulations, the more reliable the average ΔG_{TS1} and ΔG_E values obtained. Our previous computational studies[22,24] demonstrated that the average energetic results calculated by using five different starting structures (N = 5) are very close to the corresponding average results calculated by using 10 different starting structures (N = 10), suggesting that the use of five different starting structures in the FEP simulations on the BChE-cocaine systems is adequate.

Depicted in Figure 3 is the MD-simulated TS1 structure of the A199S/A328W/Y332G mutant (unperturbed TS1 structure) in comparison with the perturbed TS1 structure of the A199S/F227A/A328W/Y332G mutant. Indicated in the figure are the locations of the mutated residue #227 relative to (−)-cocaine, along with other key residues in or near the active site. The blue dashed lines represent the hydrogen bonds between the oxyanion hole (G116, G117, and S199) and the carbonyl oxygen of benzoyl ester of (−)-cocaine. F227 is dwelled on the end of the turn between two loops that form the boundary of the active site pocket of the enzyme. Following the F227A mutation (from a larger residue to a smaller one), the active site cavity became slightly larger so that it can better accommodate (−)-cocaine which is larger in molecular size than the native substrate butyrylcholine. As a result, the calculated $\Delta\Delta G(1\rightarrow2)$ value (−1.13 kcal/mol, as seen in Table 1) associated with the enzyme change A199S/A328W/Y332G → A199S/F227A/A328W/Y332G has a minus sign, which suggests that the enzyme change A199S/A328W/Y332G → A199S/F227A/A328W/Y332G should improve the catalytic efficiency of the enzyme against (−)-cocaine.

The FEP simulations on the TS1 structure associated with the enzyme changes A199S/A328W/Y332G → A199S/S287A/A328W/Y332G and A199S/S287A/A328W/Y332G → A199S/S287G/A328W/Y332G produced the perturbed TS1 structures of both the A199S/S287A/A328W/Y332G and A199S/S287G/A328W/Y332G mutants. Amino acid residue #287 is close to the benzene ring of (−)-cocaine and the S287A and A287G mutations makes more and more room and a hydrophobic environment to better accommodate the benzene ring of (−)-cocaine. Depicted in Figure 4 are the simulated TS1 structures of the A199S/A328W/Y332G and A199S/S287G/A328W/Y332G mutants for comparison. As seen in Table 1, the calculated $\Delta\Delta G(1\rightarrow2)$ value associated with the enzyme change A199S/A328W/Y332G → A199S/S287A/A328W/Y332G is −0.80 kcal/mol, and the calculated $\Delta\Delta G(1\rightarrow2)$ value associated with the enzyme change A199S/S287A/A328W/Y332G → A199S/S287G/A328W/Y332G is −0.15 kcal/mol. All of the calculated $\Delta\Delta G(1\rightarrow2)$ values have a minus sign. The cumulative $\Delta\Delta G(1\rightarrow2)$ value associated with the enzyme change A199S/A328W/Y332G → A199S/S287G/A328W/Y332G is −0.95 kcal/mol, which suggests that the enzyme change A199S/A328W/Y332G → A199S/S287G/A328W/Y332G should improve the catalytic efficiency of the enzyme against (−)-cocaine.

Similar to the FEP simulations on the F227A mutation associated with the enzyme change A199S/A328W/Y332G → A199S/F227A/A328W/Y332G, the FEP simulations on the F227A mutation associated with the enzyme change A199S/S287G/A328W/Y332G → A199S/F227A/S287G/A328W/Y332G also revealed that the perturbed TS1 structure (see Figure 5) has more room to better accommodate (−)-cocaine in the active site. As a result,

NIH-PA Author Manuscript

NIH-PA Author Manuscript

NIH-PA Author Manuscript

the calculated $\Delta\Delta G(1\rightarrow2)$ value associated with the enzyme change A199S/S287G/A328W/Y332G → A199S/F227A/S287G/A328W/Y332G is −1.05 kcal/mol, suggesting that the enzyme change A199S/S287G/A328W/Y332G → A199S/F227A/S287G/A328W/Y332G should also improve the catalytic efficiency of the enzyme against (−)-cocaine.

As seen in Table 1, the $\Delta\Delta G(1\rightarrow2)$ values associated with enzyme changes (4) – (7) were all predicted to have a minus sign, which suggests that all of the mutations associated with the enzyme changes (4) – (7) can improve the catalytic efficiency of the enzyme against (−)-cocaine. The FEP results are supported by our experimentally determined kinetic parameters. Summarized in Table 2 are the kinetic parameters determined by using the same experimental protocol. For comparison between the experimental and computational results, both the experimentally derived and FEP-calculated $\Delta\Delta G$ values are listed in Table 2 as the (cumulative) $\Delta\Delta G$ values associated with the enzyme change from the A199S/A328W/Y332G mutant to the mutant (*i.e*. A199S/F227A/A328W/Y332G, A199S/S287G/A328W/Y332G, or A199S/F227A/S287G/A328W/Y332G) under consideration. As one can see in Table 2, all of these enzyme changes have significantly improved the catalytic efficiency against (−)-cocaine. The experimental kinetic data are all qualitatively consistent with the computational results based on the FEP simulations. Quantitatively, for the enzyme change A199S/A328W/Y332G → A199S/F227A/A328W/Y332G, the experimentally derived $\Delta\Delta G$ value of −0.83 kcal/mol is close to the FEP-calculated $\Delta\Delta G$ value of −1.13 kcal/mol; the deviation is 0.30 kcal/mol. For the enzyme change A199S/A328W/Y332G → A199S/S287G/A328W/Y332G, the experimentally derived $\Delta\Delta G$ value of −1.55 kcal/mol is also reasonably close to the FEP-calculated $\Delta\Delta G$ value of −0.95 kcal/mol, with a slightly larger deviation of 0.60 kcal/mol. For the enzyme change A199S/S287G/A328W/Y332G → A199S/F227A/S287G/A328W/Y332G, the experimentally derived $\Delta\Delta G$ value of −1.92 kcal/mol is very close to the FEP-calculated $\Delta\Delta G$ value of −2.00 kcal/mol; the deviation is only 0.08 kcal/mol.

Conclusion

We have employed a unified computational approach based on free energy perturbation (FEP) simulations of transition states to examine the mutation-caused shifts of the free energy change from the free enzyme to the rate-determining transition state for (−)-cocaine hydrolysis catalyzed by a promising series of mutants of human butyrylcholinesterase (BChE), including the A199S/A328W/Y332G, A199S/F227A/A328W/Y332G, A199S/S287G/A328W/Y332G, and A199S/F227A/S287G/A328W/Y332G mutants. The FEP simulations were followed by Michaelis-Menten kinetics analysis determining the individual k_{cat} and K_M values missing for the A199S/F227A/A328W/Y332G mutant in this series. The experimental kinetic data are all qualitatively consistent with the computational results based on the FEP simulations. Quantitatively, for the enzyme change A199S/A328W/Y332G → A199S/F227A/A328W/Y332G, the FEP-calculated $\Delta\Delta G$ value of −1.13 kcal/mol is close to the experimentally derived $\Delta\Delta G$ value of −0.83 kcal/mol; the deviation is 0.30 kcal/mol. For the enzyme change A199S/A328W/Y332G → A199S/S287G/A328W/Y332G, the FEP-calculated $\Delta\Delta G$ value of −0.95 kcal/mol is also reasonably close to the experimentally derived $\Delta\Delta G$ value of −1.55 kcal/mol, with a slightly larger deviation of 0.60 kcal/mol. For the enzyme change A199S/S287G/A328W/Y332G → A199S/F227A/S287G/A328W/Y332G, the FEP-calculated $\Delta\Delta G$ value of −2.00 kcal/mol is very close to the experimentally derived $\Delta\Delta G$ value of −1.92 kcal/mol; the deviation is only 0.08 kcal/mol. The reasonable agreement between the computational and experimental data suggests that the unified computational approach based on the FEP simulations of the transition states may be valuable for future computational design of new BChE mutants with a further improved catalytic efficiency against (−)-cocaine.

NIH-PA Author Manuscript

NIH-PA Author Manuscript

NIH-PA Author Manuscript

Supplementary Material

Refer to Web version on PubMed Central for supplementary material.

Acknowledgments

This work was supported by NIH (grants R01 DA013930, R01 DA025100, and R01 DA021416). The entire work was carried out at University of Kentucky. Wenchao Yang worked in Zhan's lab at University of Kentucky as an exchange graduate student (2005–2009) or a postdoctoral fellow (since January 2010) from Central China Normal University. The authors also acknowledge the Center for Computational Sciences (CCS) at University of Kentucky for supercomputing time on an IBM X-series Cluster with 340 nodes or 1,360 processors.

References

1. Mendelson JH, Mello NK. New Engl J Med. 1996; 334:965–972. [PubMed: 8596599]
2. Singh S. Chem Rev. 2000; 100:925–1024. [PubMed: 11749256]
3. Paula S, Tabet MR, Farr CD, Norman AB, Ball WJ Jr. J Med Chem. 2004; 47:133–142. [PubMed: 14695827]
4. Gorelick DA. Drug Alcohol Depend. 1997; 48:159–165. [PubMed: 9449014]
5. Redish AD. Science. 2004; 306:1944–1947. [PubMed: 15591205]
6. Meijler MM, Kaufmann GF, Qi LW, Mee JM, Coyle AR, Moss JA. J Am Chem Soc. 2005; 127:2477–2484. [PubMed: 15725002]
7. Carrera MRA, Kaufmann GF, Mee JM, Meijler MM, Koob GF, Janda KD. Proc Natl Acad Sci USA. 2004; 101:10416–10421. [PubMed: 15226496]
8. Landry DW, Zhao K, Yang GXQ, Glickman M, Georgiadis TM. Science. 1993; 259:1899–1901. [PubMed: 8456315]
9. Zhan CG, Deng SX, Skiba JG, Hayes BA, Tschampel SM, Shields GC, Landry DW. J Comput Chem. 2005; 26:980–986. [PubMed: 15880781]
10. Kamendulis LM, Brzezinski MR, Pindel EV, Bosron WF, Dean RA. J Pharmacol Exp Ther. 1996; 279:713–717. [PubMed: 8930175]
11. Sun H, Pang YP, Lockridge O, Brimijoin S. Mol Pharmacol. 2002; 62:220–224. [PubMed: 12130672]
12. Hamza A, Cho H, Tai HH, Zhan CG. J Phys Chem B. 2005; 109:4776–4782. [PubMed: 16851561]
13. Gateley SJ. Biochem Pharmacol. 1991; 41:1249–1254. [PubMed: 2009099]
14. Darvesh S, Hopkins DA, Geula C. Nature Rev Neurosci. 2003; 4:131–138. [PubMed: 12563284]
15. Giacobini, E. Butyrylcholinesterase: Its Function and Inhibitors. Dunitz Martin Ltd; Great Britain: 2003.
16. Gao D, Zhan CG. Proteins. 2006; 62:99–110. [PubMed: 16288482]
17. Gao D, Zhan CG. J Phys Chem B. 2005; 109:23070–23076. [PubMed: 16854005]
18. Gao D, Cho H, Yang W, Pan Y, Yang GF, Tai HH, Zhan CG. Angew Chem Int Ed. 2006; 45:653–657.
19. Zhan CG, Zheng F, Landry DW. J Am Chem Soc. 2003; 125:2462–2474. [PubMed: 12603134]
20. Zhan CG, Gao D. Biophysical Journal. 2005; 89:3863–3872. [PubMed: 16319079]
21. Pan Y, Gao D, Yang W, Cho H, Yang GF, Tai HH, Zhan CG. Proc Natl Acad Sci USA. 2005; 102:16656–16661. [PubMed: 16275916]
22. Pan Y, Gao D, Yang W, Cho H, Zhan CG. J Am Chem Soc. 2007; 129:13537–13543. [PubMed: 17927177]
23. Zheng F, Yang W, Ko MC, Liu J, Cho H, Gao D, Tong M, Tai HH, Woods JH, Zhan CG. J Am Chem Soc. 2008; 130:12148–12155. [PubMed: 18710224]
24. Yang W, Pan Y, Zheng F, Cho H, Tai HH, Zhan CG. Biophysical Journal. 2009; 96:1931–1938. [PubMed: 19254552]
25. Yang, W.; Xue, L.; Fang, L.; Zhan, C-G. Chemico-Biological Interactions. 2010. in press (online version available)

NIH-PA Author Manuscript

NIH-PA Author Manuscript

NIH-PA Author Manuscript

26. Brimijoin S, Gao Y, Anker JJ. Neuropsychopharmacology. 2008; 33:2715–2725. [PubMed: 18199998]
27. Nicolet Y, Lockridge O, Masson P, Fontecilla-Camps JC, Nachon F. J Biol Chem. 2003; 278:41141–41147. [PubMed: 12869558]
28. Case, DA.; Pearlman, DA.; Caldwell, JW.; Cheatham, TE., III; Wang, J.; Ross, WS.; Simmerling, CL.; Darden, TA.; Merz, KM.; Stanton, RV.; Cheng, AL.; Vincent, JJ.; Crowley, M.; Tsui, V.; Gohlke, H.; Radmer, RJ.; Duan, Y.; Pitera, J.; Massova, I.; Seibel, GL.; Singh, UC.; Weiner, PK.; Kollman, PA. Amber7. University of California; San Francisco: 2002.
29. Frisch, MJ.; Trucks, GW.; Schlegel, HB.; Scuseria, GE.; Robb, MA.; Cheeseman, JR.; Montgomery, JA., Jr; Vreven, T.; Kudin, KN.; Burant, JC.; Millam, JM.; Iyengar, SS.; Tomasi, J.; Barone, V.; Mennucci, B.; Cossi, M.; Scalmani, G.; Rega, N.; Petersson, GA.; Nakatsuji, H.; Hada, M.; Ehara, M.; Toyota, K.; Fukuda, R.; Hasegawa, J.; Ishida, M.; Nakajima, T.; Honda, Y.; Kitao, O.; Nakai, H.; Klene, M.; Li, X.; Knox, JE.; Hratchian, HP.; Cross, JB.; Adamo, C.; Jaramillo, J.; Gomperts, R.; Stratmann, RE.; Yazyev, O.; Austin, AJ.; Cammi, R.; Pomelli, C.; Ochterski, JW.; Ayala, PY.; Morokuma, K.; Voth, GA.; Salvador, P.; Dannenberg, JJ.; Zakrzewski, VG.; Dapprich, S.; Daniels, AD.; Strain, MC.; Farkas, O.; Malick, DK.; Rabuck, AD.; Raghavachari, K.; Foresman, JB.; Ortiz, JV.; Cui, Q.; Baboul, AG.; Clifford, S.; Cioslowski, J.; Stefanov, BB.; Liu, G.; Liashenko, A.; Piskorz, P.; Komaromi, I.; Martin, RL.; Fox, DJ.; Keith, T.; Al-Laham, MA.; Peng, CY.; Nanayakkara, A.; Challacombe, M.; Gill, PMW.; Johnson, B.; Chen, W.; Wong, MW.; Gonzalez, C.; Pople, JA. Gaussian 03, Revision A.1. Gaussian, Inc; Pittsburgh, PA: 2003.
30. Jorgensen WL, Chandrasekhar J, Madura JD, Impey RW, Klein ML. J Chem Phys. 1983; 79:926.
31. Berendsen HJC, Postma JPM, van Gunsteren WF, DiNola A, Haak JR. J Chem Phys. 1984; 81:3684.
32. Ryckaert JP, Ciccotti G, Berendsen HJC. J Comput Phys. 1977; 23:327.
33. Essmann U, Perera L, Berkowitz ML, Darden T, Lee H, Pedersen LG. J Chem Phys. 1995; 103:8577.
34. Sun H, Shen ML, Pang YP, Lockridge O, Brimijoin S. J Pharmacol Exp Ther. 2002; 302:710–716. [PubMed: 12130735]
35. Rao SN, Singh UC, Bash PA, Kollman PA. Nature. 1987; 328:551–554. [PubMed: 3302725]
36. Florian J, Goodman MF, Warshel A. J Phys Chem B. 2000; 114:10092–10099.
37. Bren U, Martinek V, Florian J. J Phys Chem B. 2006; 110:10557–10566. [PubMed: 16722767]
38. Press, WH.; Flannery, BP.; Teukolsky, SA.; Vetterling, WT. Numerical Recipes in FORTRAN: The Art of Scientific Computing. 2. Cambridge, England: Cambridge University Press; 1992.
39. Hao G-F, Yang G-F, Zhan C-G. J Phys Chem B. 2010 July 6. [Epub ahead of print].

NIH-PA Author Manuscript

NIH-PA Author Manuscript

NIH-PA Author Manuscript

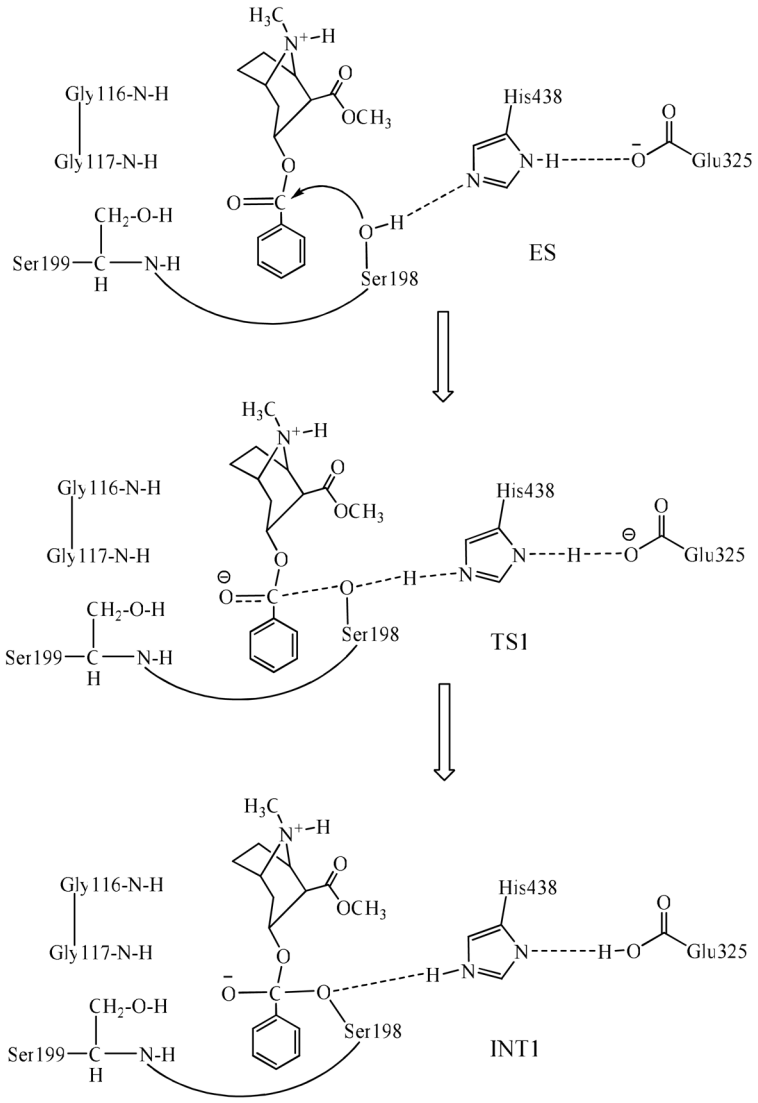

Figure 1.
Schematic representation of the first reaction step of the chemical reaction process for (−)-cocaine hydrolysis catalyzed by BChE mutant including the A199S mutation.

NIH-PA Author Manuscript

NIH-PA Author Manuscript

NIH-PA Author Manuscript

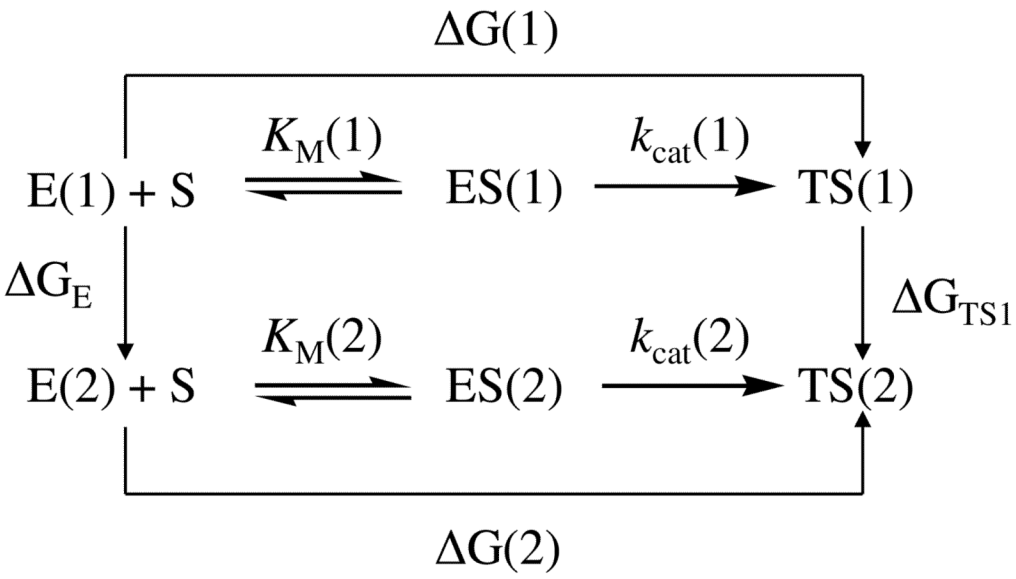

Figure 2.

The relationship between different free energy changes for the reactions catalyzed by two enzymes. E(*i*) is the free enzyme, ES(*i*) represents the enzyme-substrate complex, and TS1(*i*) refers to the transition state. $\Delta G(i)$ is the sum of the enzyme-substrate binding free energy $\Delta G_{ES}(i)$ and the activation free energy $\Delta G_{av}(i)$ (i = 1, 2).

NIH-PA Author Manuscript
NIH-PA Author Manuscript
NIH-PA Author Manuscript

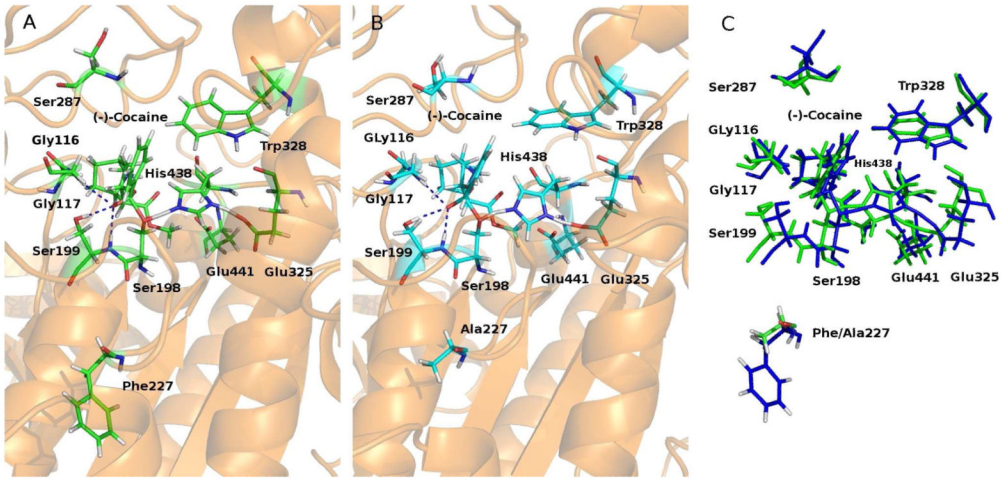

Figure 3.

(A) The simulated TS1 structure associated with the A199S/A328W/Y332G mutant. The dashed lines in blue indicate the hydrogen bonds between (−)-cocaine and the oxyanion hole of the mutant. (B) The simulated TS1 structure associated with the A199S/F227A/A328W/Y332G mutant. (C) Superimposition of the two TS1 structures associated with the A199S/A328W/Y332G (green) and A199S/F227A/A328W/Y332G mutants (blue).

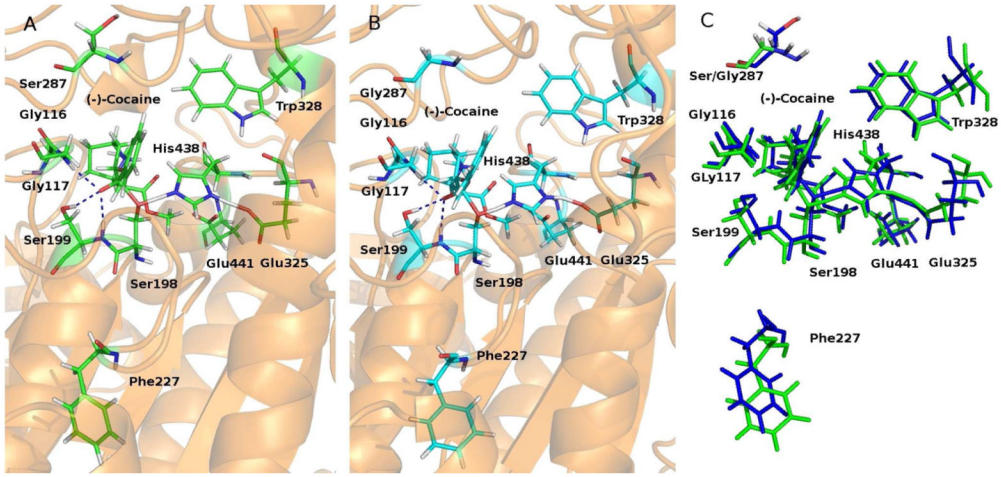

Figure 4.

(A) The simulated TS1 structure associated with the A199S/A328W/Y332G mutant. The dashed lines in blue indicate the hydrogen bonds between (−)-cocaine and the oxyanion hole of the mutant. (B) The simulated TS1 structure associated with the A199S/S287G/A328W/Y332G mutant. (C) Superimposition of the two TS1 structures associated with the A199S/A328W/Y332G (*green*) and A199S/S287G/A328W/Y332G mutants (blue).

NIH-PA Author Manuscript NIH-PA Author Manuscript NIH-PA Author Manuscript

NIH-PA Author Manuscript

NIH-PA Author Manuscript

NIH-PA Author Manuscript

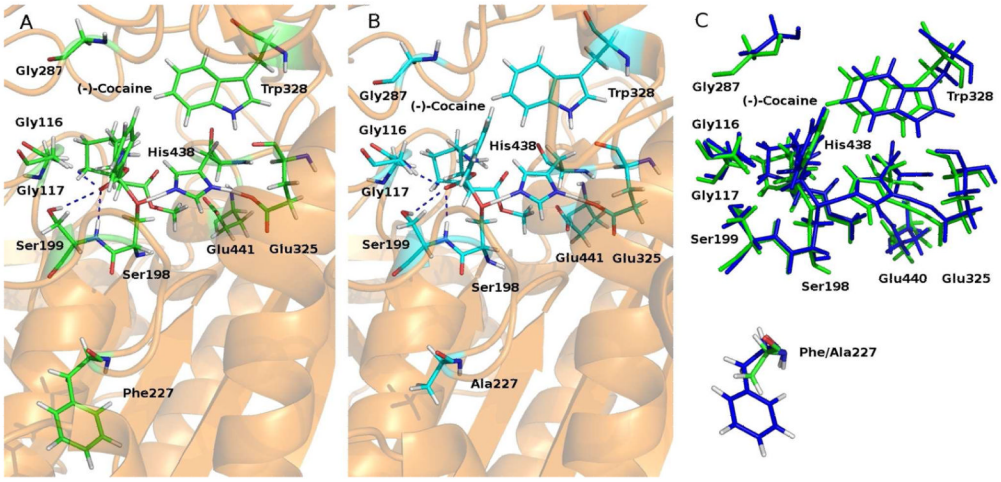

Figure 5.

(A) The simulated TS1 structure associated with the A199S/S287G/A328W/Y332G mutant. The dashed lines in blue indicate the hydrogen bonds between (−)-cocaine and the oxyanion hole of the mutant. (B) The simulated TS1 structure associated with the A199S/F227A/S287G/A328W/Y332G mutant. (C) Superimposition of the two TS1 structures associated with the A199S/S287G/A328W/Y332G (green) and A199S/F227A/S287G/A328W/Y332G mutants (blue).

NIH-PA Author Manuscript

NIH-PA Author Manuscript

NIH-PA Author Manuscript

Table 1

The FEP-calculated free energy changes (in kcal/mol) in comparison with the experimental kinetic data for (−)-cocaine hydrolysis catalyzed by BChE mutants.

Mutation	ΔG_E[a]	ΔG_{TS1}[a]	$\Delta\Delta G(1\rightarrow2)$
A199S/A328W/Y332G → A199S/F227A/A328W/Y332G	6.12 (0.29)	4.98 (0.25)	−1.13
A199S/A328W/Y332G → A199S/S287A/A328W/Y332G	8.58 (0.16)	7.78 (0.50)	−0.80
A199S/S287A/A328W/Y332G → A199S/S287G/A328W/Y332G	−5.67 (0.54)	−5.82 (0.52)	−0.15
A199S/S287G/A328W/Y332G → A199S/F227A/S287G/A328W/Y332G	6.85 (0.44)	5.80 (0.51)	−1.05
A199S/A328W/Y332G → A199S/S287G/A328W/Y332G[b]	2.91	1.96	−0.95
A199S/A328W/Y332G → A199S/F227A/S287G/A328W/Y332G[c]	9.76	7.76	−2.00

[a] ΔG_E and ΔG_{TS1} are the mutation-caused free energy changes for the free enzyme and transition state, respectively. The number in the parenthesis after the ΔG_E or ΔG_{TS1} value refers to the root-mean-square fluctuation (RMSF) of the ΔG_E or ΔG_{TS1} values calculated starting from the five initial structures. The corresponding standard error (SE) can be estimated from the RMSF value by using Eq. (8) and N = 5, *i.e.* SE = RMSF/2.236.

[b] The theoretical results were derived from the FEP results obtained for the enzyme changes A199S/A328W/Y332G → A199S/S287A/A328W/Y332G → A199S/S287G/A328W/Y332G.

[c] The theoretical results were derived from the FEP results obtained for the enzyme changes A199S/A328W/Y332G → A199S/S287A/A328W/Y332G → A199S/S287G/A328W/Y332G → A199S/F227A/S287G/A328W/Y332G.

NIH-PA Author Manuscript NIH-PA Author Manuscript NIH-PA Author Manuscript

Table 2

Experimental kinetic data in comparison with the FEP-calculated cumulative free energy shifts (in kcal/mol) of the free energy change from the free enzyme to the rate-determining transition state for (−)-cocaine hydrolysis catalyzed by the BChE mutants.

Mutant	Experiment kinetic data					Calc.
	k_{cat} (min^{-1})	K_M (μM)	k_{cat}/K_M ($min^{-1}M^{-1}$)	Relative k_{cat}/K_M[f]	ΔΔG[g]	ΔΔG[h]
Wild-type BChE[a]	4.1	4.5	9.1×10^5	1	N.A.[i]	N.A.[i]
A199S/A328W/Y332G[b]	389	5.4	7.2×10^7	79	0.00	0.00
A199S/F227A/A328W/Y332G[c]	1150	3.9	3.0×10^8	320	−0.83	−1.13
A199S/S287G/A328W/Y332G[d]	3060	3.1	9.9×10^8	1080	−1.55	−0.95
A199S/F227A/S287A/A328W/Y332G[e]	5700	3.1	1.8×10^9	2020	−1.92	−2.00

[a] The experimental data from ref. 11

[b] The experimental data from ref. 22

[c] The kinetic parameters determined in this study

[d] The experimental data from ref. 24

[e] The experimental data from ref. 23

[f] The relative k_{cat}/K_M refers to the ratio of the catalytic efficiency of the BChE mutant to that of the wild-type against (−)-cocaine.

[g] The experimentally-derived cumulative ΔΔ*G* from the A199S/A328W/Y332G mutant to the mutant under consideration.

[h] The computationally determined cumulative ΔΔ*G* from the A199S/A328W/Y332G mutant to the mutant under consideration.

[i] N.A., Not applicable.